

# Fiber Bragg grating strain modulation based on nonlinear string transverse-force amplifier

Kuo Li,<sup>1,\*</sup> Man Hong Yau,<sup>1</sup> Tommy H. T. Chan,<sup>1</sup> David Thambiratnam,<sup>1</sup> and Hwa Yaw Tam<sup>2</sup>

<sup>1</sup>Civil Engineering and Built Environment, Queensland University of Technology, Brisbane 4000, Australia

<sup>2</sup>Photonic Research Centre, The Hong Kong Polytechnic University, Hong Kong, China

\*Corresponding author: tolikuo@gmail.com

Received November 14, 2012; revised December 5, 2012; accepted December 5, 2012;  
posted December 7, 2012 (Doc. ID 179901); published January 22, 2013

The only effective method of fiber Bragg grating (FBG) strain modulation has been by changing the distance between its two fixed ends. We demonstrate an alternative that is more sensitive to force based on the nonlinear amplification relationship between a transverse force applied to a stretched string and its induced axial force. It may improve the sensitivity and size of an FBG force sensor, reduce the number of FBGs needed for multiaxial force monitoring, and control the resonant frequency of an FBG accelerometer. © 2013 Optical Society of America  
OCIS codes: 060.3735, 060.2370.

A fiber Bragg grating (FBG) is inherently sensitive to strain and temperature by changing its resonant wavelength [1]. With intrinsic advantages of frequency modulation, ease of multiplexing, and strong immunity to electromagnetic interference, FBG strain-modulated equipment is well suited for many fields, such as structural health monitoring [2], seismic monitoring, and telecommunication [3,4].

However, the only effective method to modulate FBG's strain evenly has been by changing the distance between its fixed ends [3–10]. The method was proposed early [3] and demonstrated [4] to compensate for FBG inherent temperature sensitivity for a wavelength filter by using bimetallic strain change with temperature. Different temperature sensitivities have also been achieved based on the similar theories [6–8]. Besides converting the strain or displacement of the bonded object of an FBG, the method has also been used to directly convert an axial force to the strain change of a stretched FBG [9,10]. Other methods, however, are either obsolete or with evident side effects. For example, epoxying an FBG throughout to a surface and bending the surface to modulate its strain unevenly can eliminate temperature influence by changing the reflected power instead of the resonant wavelength, but is no longer frequency modulation [11].

Alternatively, applying a transverse force to a stretched FBG can modulate its strain evenly and more efficiently in terms of the force needed to induce the same strain change, because it can induce a stronger axial force along the FBG and therefore a larger strain change.

Figure 1 shows the mechanism of the amplification. A vertically moving rod with a round, frictionless top pulls a horizontally stretched string fixed by its two ends from point C to point C'. Assume that the distance between the two points CC' is  $y$ , and the angles formed are  $\alpha$  and  $\beta$ . Because there is no friction at the point C', the string can move freely from one side to the other side there, and the magnitudes of the axial forces and strains are the same between the two sides.

In the vertical direction of the point C' of the string,  $F_t = (F_l + \Delta F_l)(\sin \alpha + \sin \beta) = AE(\varepsilon + \Delta \varepsilon)(\sin \alpha + \sin \beta)$ , where  $F_t$ ,  $F_l$ ,  $\Delta F_l$ ,  $\varepsilon$ ,  $\Delta \varepsilon$ ,  $A$ , and  $E$  are the vertical projection of  $F_r$  (the force applied by the rod), original

axial force, induced axial force by  $F_t$ , prestrain, induced strain, cross-sectional area, and Young's modulus of the string, respectively;

$$\Delta \varepsilon = \frac{\sqrt{x^2 + y^2} + \sqrt{(L-x)^2 + y^2} - L}{L}, \quad (1)$$

where  $L$  is the distance between the two fixed ends of the string and  $x$  is the distance between the point C and one end of the string. So the amplification of the transverse force  $F_t$  is

$$\frac{\Delta F_l}{F_t} = \frac{\Delta \varepsilon}{(\varepsilon + \Delta \varepsilon) \left( \frac{y}{\sqrt{x^2 + y^2}} + \frac{y}{\sqrt{(L-x)^2 + y^2}} \right)}. \quad (2)$$

When the transverse is applied at the middle ( $x = 0.5L$ ),  $F_t = \frac{2AE(\varepsilon + \Delta \varepsilon)\sqrt{2\Delta \varepsilon + \Delta \varepsilon^2}}{\Delta \varepsilon + 1}$ , and  $\frac{\Delta F_l}{F_t} = \frac{\Delta \varepsilon(\Delta \varepsilon + 1)}{2(\varepsilon + \Delta \varepsilon)\sqrt{2\Delta \varepsilon + \Delta \varepsilon^2}}$ . When  $\Delta \varepsilon \leq 1\%$ , they can be approximately represented as  $F_t \approx 2\sqrt{2}AE(\varepsilon + \Delta \varepsilon)\Delta \varepsilon^{1/2}$  and  $\frac{\Delta F_l}{F_t} \approx \frac{\sqrt{2}\Delta \varepsilon^{1/2}}{4\varepsilon + 4\Delta \varepsilon}$ , and the errors are less than 0.75%. When  $\varepsilon \gg \Delta \varepsilon$ ,  $\frac{\Delta F_l}{F_t} \approx \frac{\sqrt{2}\Delta \varepsilon^{1/2}}{4\varepsilon} \approx \frac{F_t}{8AE\varepsilon^2}$ . When  $\varepsilon \ll \Delta \varepsilon$ ,  $\frac{\Delta F_l}{F_t} \approx \frac{\sqrt{2}\Delta \varepsilon^{1/2}}{4\Delta \varepsilon} \approx \frac{(AE)^{1/3}}{2F_t^{1/3}}$ .

The FBG's resonant wavelength shift induced by its strain change is  $\Delta \lambda = \lambda(1 - P_e)\Delta \varepsilon = \lambda(1 - P_e)\frac{\Delta F_l}{AE}$ , where  $\lambda$  is the original resonant wavelength and  $P_e$  is the photo-elastic constant.

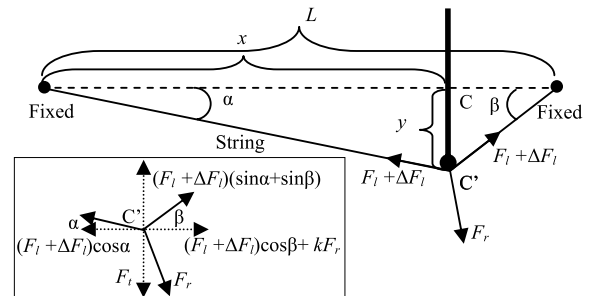


Fig. 1. Transverse force applied to a stretched string. The inset is the force diagram of the point C' of the string.

Theoretically, 0.1 N transverse force applied at the middle of a scarcely stretched FBG will induce 1.03 N axial force as  $\frac{\Delta F_t}{F_t} \approx \frac{(AE)^{1/3}}{2F_t^{1/3}}$  and 1.47 nm resonant wavelength shift as  $\Delta\lambda = \lambda(1 - P_e) \frac{\Delta F_t}{AE}$ , taking typical values of FBG for  $AE$  846.76 N ( $3.1416 * (0.125/2)^2 * 6.9 * 10^{10}$ ),  $P_e$  0.22, and  $\lambda$  1550 nm. Because the resonant wavelength shift is 10.3 times larger than what 0.1 N axial force induces, the FBG is 10.3 times more sensitive to 0.1 N transverse force and the nonlinear sensitivity of such an FBG force sensor is improved as many times as the amplification of the transverse force.

The optimum for the largest amplification is that the prestrain is negligible and the transverse force is the smallest as  $\frac{\Delta F_t}{F_t} \approx \frac{(AE)^{1/3}}{2F_t^{1/3}}$ , and the applied position is at the middle because of the symmetry of this problem and the results shown in Fig. 4. Theoretically, the amplification is infinite for an infinitesimal force at zero prestrain. It might be significant in reducing the sizes of the cumbersome strain sensors for detecting extremely low signals such as gravitational waves [12]. The amplification becomes less evident and finally an increasing diminishment as  $\Delta\epsilon$  increases.

In its horizontal direction,  $(F_t + \Delta F_t) \cos \alpha = (F_t + \Delta F_t) \cos \beta + kF_r$ , where  $kF_r$  is the horizontal projection of  $F_r$ . When  $\alpha$  and  $\beta$  are small,  $\cos \alpha \approx \cos \beta$  and  $kF_r \approx 0$ . The closer to the middle the applied position, the smaller  $kF_r$ . For example, when  $x = 0.65L$  and 1% more strain change has been induced than that at its horizontal state,  $y = 0.06769L$  according to Eq. (1),  $\cos \alpha = 0.65 / \sqrt{0.65^2 + 0.06769^2} = 0.995$ ,  $\cos \beta = 0.982$ , and  $kF_r = 0.013(F_t + \Delta F_t)$ . 64.7% ( $\sqrt{0.65^2 + 0.06769^2}L = 0.6535L$ ) of the string is at the left and 35.3% ( $0.3565L$ ) is at the right. 0.3% ( $0.0030L$ ) has moved from the left to the right.

The Bragg gratings used in the experiments were manufactured on bending insensitive fibers (Silibend G.657.B, Silitec Fibers Ltd.) by using phase masks, ~6 mm in length, ~0.2 nm of 3 dB bandwidth, and ~90% of reflectivity. A wavelength interrogator (SM130, Micronoptics Ltd.) based on a Fabry–Perot cavity with a repeatability of 1 pm and an electrical mass scale with a resolution of 0.01 g were used.

Figure 2 shows the experimental setups, in which the free-state resonant wavelength of the only FBG used was ~1535.57 nm at room temperature. In the axial-force-wavelength experiment, an object was glued at one end of the FBG far from the Bragg grating, and the other end was lifted by hand. More weights were hung on the object to test its response. In the strain-wavelength experiment, the two ends of the FBG were epoxied on the two pillars of a horizontal stretching stage with a resolution of 0.01 mm. The position of one pillar was adjustable by screws. The distance between the two fixed ends of the FBG was 99.75 mm at its initial stretching position, measured by a digital vernier caliper with a resolution of 0.01 mm. Different displacements of the adjustable pillar were given by tuning the screw to test its response. Figure 3 shows the results of these two experiments, from which  $AE = 1159.02 \text{ nm}/1.33 \text{ nm/N} = 871.44 \text{ N}$  and  $P_e = 1 - 1159.02 \text{ nm}/1535.57 \text{ nm} = 0.25$ .

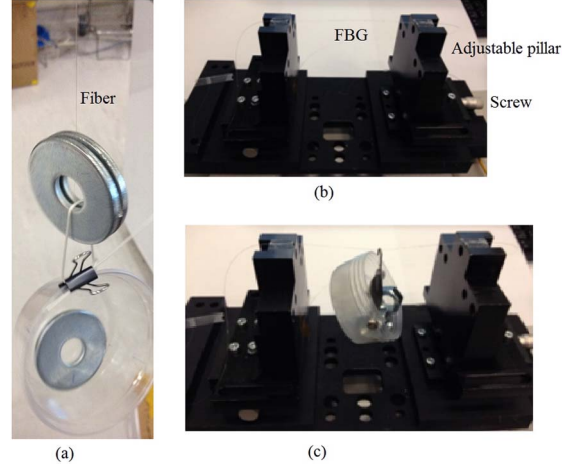


Fig. 2. (Color online) Setups of the axial-force-wavelength (a), strain-wavelength (b), and transverse-force wavelength (c) experiments.

Its transverse-force-wavelength response was tested at  $x = 0.5L$  and  $0.35L$  with different prestretches (~0.05, ~0.6, ~1.2, and ~1.8 nm resonant wavelength shifts from its free state), by using the above stretching stage to hold and prestretch the FBG as shown in Fig. 2(c). Different transverse forces were applied by hanging a basket weighted ~0.1 N on the FBG and putting four objects weighted ~0.15 N each into the basket one by one to test its response. The applied positions were measured by the above digital vernier caliper, and the experiment was repeated three times.

Viewing the basket and string as a whole, in the horizontal and vertical directions, we have  $F_{\text{left}} \cos \alpha = F_{\text{right}} \cos \beta$ ,  $\cos \alpha \approx \cos \beta$ ,  $F_{\text{left}} \approx F_{\text{right}}$ ;  $F_{\text{left}} \sin \alpha + F_{\text{right}} \sin \beta = F_t$ , where  $F_{\text{left}}$  and  $F_{\text{right}}$  are the axial forces of the left and right sides, respectively. Although this setup is slightly different from Fig. 1, equations in its vertical direction are still applicable because  $F_{\text{left}} \approx F_{\text{right}}$  and the strains of the two sides are still almost the same. Theoretically, when  $x = 0.65L$  and 1% more strain change is induced, because the string cannot move at the applied position and the length ratio of the two sides cannot change, unlike that in Fig. 1, the basket

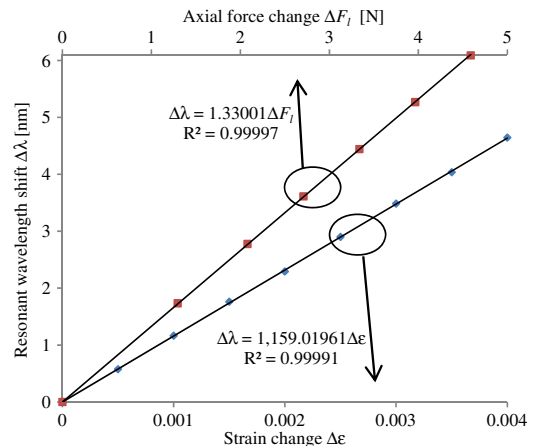


Fig. 3. (Color online) Axial-force-wavelength and strain-wavelength responses of an FBG.

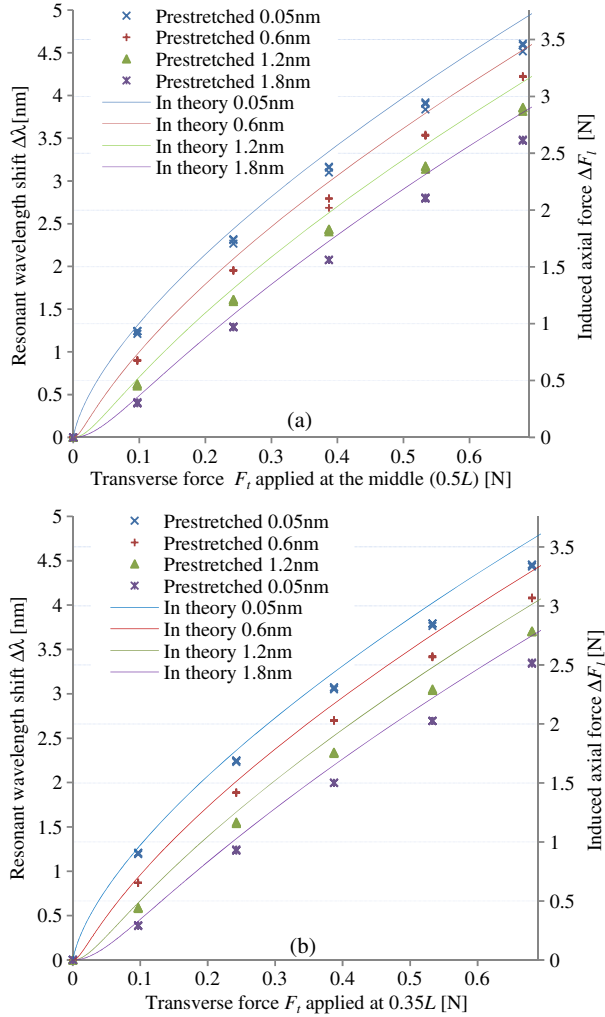


Fig. 4. (Color online) Amplification of the transverse forces applied to an FBG at the middle ( $0.5L$ ) (a) and  $0.35L$  (b) with different prestretches.

will move to the right for a distance  $\sim 0.003L$  to make  $F_{\text{left}} \approx F_{\text{right}} \cdot \cos \alpha \approx (0.65 + 0.003)/(0.65 * 1.01) = 0.995$  and  $\cos \beta \approx 0.982$ .

The experimental results are shown in Fig. 4, in which the transverse forces are compared with their induced axial forces by converting the observed resonant wavelength shifts to the axial force changes based on  $\Delta\lambda = 1.33001\Delta F_l$  shown in Fig. 3. The theoretical predictions were calculated based on Eqs. (1) and (2) by designating an increasing  $y$ . The experimental results were slightly lower than the theoretical ones, which probably stemmed from the tiny tilt and displacement of the adjustable pillar where one end of the FBG was fixed. The applied positions were between the Bragg grating and interrogator, and the powers of the resonant waves fluctuated within 2% during the experiment, but showed no dependence on the transverse forces.

0.10 and 0.68 N transverse forces applied at the middle ( $0.5L$ ) were amplified 9.60 and 5.05 times on

average with  $\sim 0.05$  nm prestretch (prestrain:  $\sim 0.05$  nm/1159.02 nm =  $\sim 0.00004$ ), while only being amplified 3.15 and 3.84 times on average with  $\sim 1.8$  nm prestretch, respectively. When they were applied at  $0.35L$ , the above figures changed to 9.33 and 4.91 times with  $\sim 0.05$  nm prestretch and 3.01 and 3.70 times with  $\sim 1.8$  nm prestretch, respectively. This shows that the prestrain has a very strong influence on the nonlinear amplification, while the applied position does not. Therefore, the nonlinear results of such equipment are easier to process if their prestrains are negligibly small.

The number of FBGs needed for multiaxial force measurement may be reduced. For example, the biaxial inclinometer [9] may be achieved by two FBGs instead of four. A surface supporting the inertial mass is necessary for applying the biaxial forces according to inclinations. The axial inclinations were distinguished by the differentials between the resonant wavelengths of the two FBGs, while the transverse inclinations may now be calculated.

The resonant frequency of such an FBG accelerometer may be controlled by changing its prestrain, the length between its fixed ends, or the mass of its inertial object. We will report this elsewhere.

In conclusion, we theoretically proved that applying a transverse force to a stretched string can induce a stronger axial force and, in the case of a stretched FBG, a larger resonant wavelength shift. In the experiments, the FBG's resonant wavelength responses to axial and transverse forces were tested and compared, which validated the theoretical predictions. Some advantages of this strain modulation method were also discussed.

We thank the reviewers for the helpful comments. K. Li and M. H. Yau acknowledge the doctorate scholarships provided by Queensland University of Technology. This work was also supported by grants from the Research Grants Council of the Hong Kong SAR, China (RGC Ref. No. 512006).

## References

1. B. Lee, *Opt. Fiber Technol.* **9**, 57 (2003).
2. M. Jones, *Nat. Photonics* **2**, 153 (2008).
3. W. W. Morey and W. L. Glomb, "Incorporated Bragg filter temperature compensated optical waveguide device," U.S. patent 5,042,898 (August 27, 1991).
4. G. W. Yoffe, P. A. Krug, F. Ouellette, and D. A. Thorncraft, *Appl. Opt.* **34**, 6859 (1995).
5. A. Stefani, S. Andresen, W. Yuan, N. Herholdt-Rasmussen, and O. Bang, *IEEE Photon. Technol. Lett.* **24**, 763 (2012).
6. J. Jung, H. Nam, B. Lee, J. O. Byun, and N. S. Kim, *Appl. Opt.* **38**, 2752 (1999).
7. K. Li, Z. A. Zhou, and A. Liu, *Chin. Opt. Lett.* **7**, 121 (2009).
8. K. Li and Z. A. Zhou, *Chin. Opt. Lett.* **7**, 191 (2009).
9. H. Y. Au, S. K. Khijwania, H. Y. Fu, W. H. Chung, and H. Y. Tam, *J. Lightwave Technol.* **29**, 1714 (2011).
10. H. J. Chen, L. Wang, and W. F. Liu, *Appl. Opt.* **47**, 556 (2008).
11. X. Y. Dong, X. F. Yang, C. L. Zhao, L. Ding, P. Shum, and N. Q. Ngo, *Smart Mater. Struct.* **14**, N7 (2005).
12. D. Reitze, *Nat. Photonics* **2**, 582 (2008).